ACS Sustainable Chemistry & Engineering

Research Article

Cite This: ACS Sustainable Chem. Eng. 2018, 6, 11819−11826

pubs.acs.org/journal/ascecg

Four Atom Efficient Enzyme Cascades for All 4-Methoxyphenyl-1,2-propanediol Isomers Including Product Crystallization Targeting High Product Concentrations and Excellent *E*-Factors

Reinhard Oeggl,[†,∥] Tim Maßmann,[‡,∥] Andreas Jupke,[‡] and Dörte Rother*[,†,§]

[†]IBG-1: Biotechnology, Forschungszentrum Jülich GmbH, Wilhelm Johnen Straße, 52425 Jülich, Germany

[‡]Aachener Fluidverfahrenstechnik, RWTH Aachen University, Forckenbeckstraße 51, 52074 Aachen, Germany

[§]Aachen Biology and Biotechnology, RWTH Aachen University, Worringerweg 1, 52074 Aachen, Germany

Supporting Information

ABSTRACT: Atom economy and *E*-factor calculations are valuable tools in the sustainable process design of fine and pharmaceutical chemicals. Adjoined with the smart assembly of biocatalysts in artificial cascades, fine and pharmaceutical chemicals can be produced with high efficiency and selectivity, while also reducing the ecological footprint. In this study, all four isomers of 4-methoxyphenyl-1,2-propanediol, a potential anti-inflammatory drug, are synthesized by stereocomplementary carboligases and NADPH-dependent alcohol dehydrogenases in a one-pot, two-step cascade with isomeric purities of >99%. The consumed NADPH in the second step is regenerated by the same alcohol dehydrogenase (ADH) with an auxiliary substrate, which allows coproduct recycling into the first step to form a self-sufficient cascade and increase atom economy to 99.9%. In addition, a hydrophobic microaqueous reaction system (MARS) enabled space-time yields (STYs) of up to 165 g L^{-1} day^{-1} for the respective product isomers. The employment of this organic reaction environment facilitates product crystallization with an isolated yield of 38% and crystal purities of 99.9%. Crystal separation by filtration allows any required substrate surplus to be reapplied in a next batch, thus reducing the *E*-factor potentially close to 1.

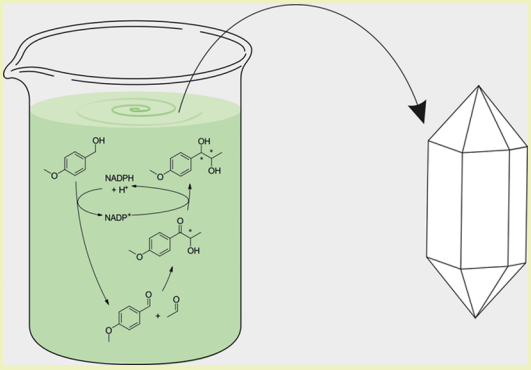

KEYWORDS: *One-pot cascade, Enzymatic cascade, Atom economy, E-factor, Product crystallization, Self-sufficient cascade, Coproduct recycling*

INTRODUCTION

The implementation of biocatalytic steps as well as product crystallization gains increased interest for a more sustainable manufacturing in organic synthesis. Especially in synthesis, biocatalysis offers the inherent advantages of high catalyst selectivity, nontoxic reaction conditions, and biodegradability, to name a few.[1] However, biocatalysis is often perceived as limited in terms of (i) satisfying space-time yields (STYs), (ii) catalyst-cost efficiency, (iii) laborious downstream processing, and (iv) the low atom economy of oxidoreductase processes.

Here, a sustainable biocatalytic process for 4-methoxyphenyl-1,2-propanediol (Figure 1, **4**), a potential pharmaceutical drug and valuable synthon for (*R*)-tamsulosin and silibinin, is presented. Currently, **4** is still obtained by either tedious extraction from plants or organic synthesis.[2−7] This organic synthesis encompasses Sharpless asymmetric dihydroxylation, epoxide hydrolysis, and asymmetric aldol condensation.[8−14] Unfortunately, the methods themselves only access racemic product mixtures and do not consider environmental factors (singular *E*-factor). The *E*-factor is the quotient of all educts to the target product, which emphasizes the waste formed per equivalent product and thus a key parameter for sustainable process design.[8−14]

The above-mentioned challenges are overcome in this study by a self-sufficient two-step, one-pot cascade design for the asymmetric synthesis of all four stereoisomers of **4** including facile product isolation by crystallization.

Four stereocomplementary cascades are assembled, starting with inexpensive 4-methoxy-benzaldehyde (**1**) and acetaldehyde (**2**).[15−17] These are ligated to the intermediate 4-methoxyphenyl-2-hydroxy-propanone (Figure 1, **3**) by either *Pseudomonas fluorescens* benzaldehyde lyase (*Pf*BAL, (*R*)-selective) or *Pseudomonas putida* benzoylformate decarboxylase variant L461A (*Pp*BFD varL461A, (*S*)-selective).[18−22] Subsequently, the intermediate is reduced at the keto position by either *Ralstonia* sp. alcohol dehydrogenase (RADH, (*R*)-selective) or *Lactobacillus brevis* alcohol dehydrogenase (*Lb*ADH, (*S*)-selective) to form **4**.[23−26]

Received: May 8, 2018
Revised: June 28, 2018
Published: July 4, 2018

DOI: 10.1021/acssuschemeng.8b02107
ACS Sustainable Chem. Eng. 2018, 6, 11819−11826

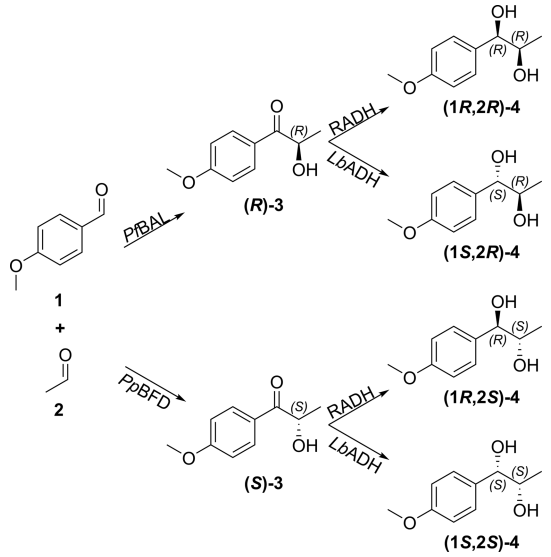

Figure 1. Stereocomplementary catalyst combinations grant access to all four 4-methoxyphenyl-1,2-propanediol isomers. 4-Methoxy-benzaldehyde (**1**), acetaldehyde (**2**), 4-methoxyphenyl-2-hydroxy-propanone (**3**), 4-methoxyphenyl-1,2-propanediol (**4**), *P. fluorescens* benzaldehyde lyase (*Pf*BAL), *P. putida* benzoylformate decarboxylase (*Pp*BFD) variant L461A, *Ralstonia* sp. alcohol dehydrogenase (RADH), and *L. brevis* alcohol dehydrogenase (*Lb*ADH).

High space-time yields (STYs) are realized by utilizing a monophasic hydrophobic environment that is easy to set up: a microaqueous reaction system (MARS). This was first introduced in 1987 and recently optimized for biocascade applications.[15,16,27] In MARS, lyophilized whole cell (LWC) catalysts are suspended in a substrate−solvent mixture. These LWCs contain high amounts of the above-described recombinant biocatalyst. The addition of a small buffer fraction hydrates LWCs and ensures catalytic activity.[15,16,28−31] This catalyst formulation provides necessary cofactors and spares cost-intensive enzyme purification.[32,33] The solvent selection proves to be essential in the MARS setup and optimization because solvents impact catalytic activity differently. In addition, the CHEM21 guidelines for the environmental and safety factors play a major role in the selection of appropriate solvents.[34,35] The established biocascades in MARS mostly rely on MTBE, a solvent recently evaluated as hazardous.[15,36,37] A thorough screening for a safe solvent was thus performed in accordance with CHEM21 guidelines.

Biocatalytic cascades with NADPH-dependent enzymes pose a challenge to atom efficiency and acceptable *E*-factors.[38−40] This could be addressed by either (i) smart cosubstrate application or (ii) a cosubstrate that allows a coproduct recycling to setup a self-sufficient cascade (Figure 2). Smart cosubstrates gain their name from the spontaneous lactone formation of their corresponsive product.[41,42] The irreversible lactone formation occurs almost immediately upon cosubstrate double oxidation and shifts the thermodynamic equilibrium to the product side. For coproduct recycling 4-methoxybenzyl alcohol (**5**) is employed as cosubstrate. The resulting 4-methoxy-benzaldehyde (**1**) is directly recycled in the first step to form a self-sufficient cascade. Both options impact an *E*-factor positively. Adjoined with selective product crystallization, any excess substrate and formed coproduct can in principle be recycled in the next batch.

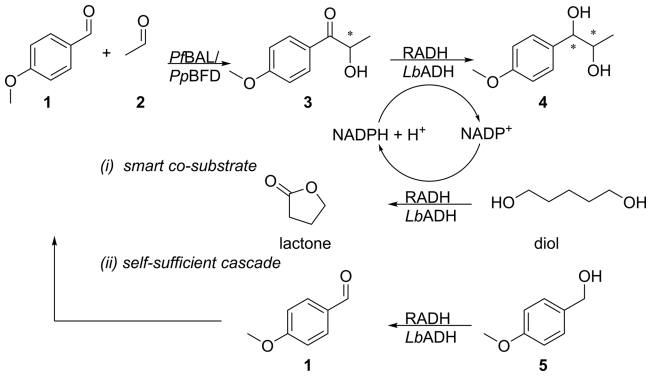

Figure 2. NADPH regeneration in (i) a parallel cascade and (ii) a self-sufficient cascade design. 4-Methoxy-benzaldehyde (**1**), acetaldehyde (**2**), 4-methoxyphenyl-2-hydroxy-propanone (**3**), 4-methoxyphenyl-1,2-propanediol (**4**), 4-methoxybenzyl alcohol (**5**). *P. fluorescens* benzaldehyde lyase (*Pf*BAL), *P. putida* benzoylformate decarboxylase (*Pp*BFD) variant L461A, *Ralstonia* sp. alcohol dehydrogenase (RADH), *L. brevis* alcohol dehydrogenase (*Lb*ADH).

The realization of high product concentrations in MARS and the avoidance of further additives in downstream isolation emphasize the potential synergetic effect that clever upstream reaction design combined with downstream product isolation has on STY and sustainable *E*-factors.

METHODS AND MATERIALS

Chemicals. 4-Methoxy-benzaldehyde (**1**), acetaldehyde (**2**), 4-methoxybenzyl alcohol (**5**), 1,5-pentanediol, 1,4-pentanediol, and 3-methyl-1,5-pentanediol were purchased from Sigma-Aldrich with purities of ≥98%. The organic solvents cyclopentyl methyl ether (CPME), methyl *tert*-butyl ether (MTBE), methyl isobutyl ketone (MIBK), and 2-methyltetrahydrofuran (MTHF), obtained from Sigma-Aldrich with purities of ≥95%, were dried with a 4 Å molecular sieve and stored in an argon atmosphere upon usage. 2-Propanol and *n*-heptane were supplied by Biosolve Chemie SARL in HPLC grade. Both enantiomers of 4-methoxyphenyl-2-hydroxy-propanone were synthesized enzymatically and purified under the same parameters described by Jakoblinnert and Rother for 2-hydroxy-phenylpropanone.[16] 4-Methoxyphenyl-1,2-propanone was chemically synthesized and purified according to Kulig et al.[10]

Biocatalyst Preparation. Lyophilized whole cells were applied as catalysts and prepared as follows: *Pf*BAL (GenBank AY007242.1) was heterologously produced in *Escherichia coli* (*E. coli*) SG13009 cells, as described elsewhere.[16] *Pp*BFD varL461A (PDB 2V3W), RADH (PDB 4BMS_A), and *Lb*ADH (GenBank CAD66648.1) were produced in *E. coli* BL21 in an autoinduction medium at 20 °C and 90 rpm for 72 h. The cell suspension was centrifuged at 4000 rcf and 4 °C for 20 min. The pellets were frozen at −20 °C and subsequently lyophilized at −54 °C and 0.01 mbar. The dried pellets were then mortared to crude powder and stored at −20 °C until usage.

Cosubstrate Substrate Selection for NADPH Regeneration. First, different cosubstrates were investigated. The 30 mg mL^{-1} RADH LWC with 45 μL mL^{-1} 1 M TEA buffer pH 10 and 400 mM (*R*)-**3** solved in CPME were tested with 0.5 M 1,5-pentanediol, 1,4-pentanediol, 3-methyl-1,5-pentanediol, and 1 M **5** at 30 °C and 1000 rpm. The experimental setup was performed analogously with 30 mg mL^{-1} *Lb*ADH LWC and 15 μL mL^{-1} 1 M TEA buffer pH 10.

Second, different concentrations of **5**, 30 mg mL^{-1} RADH LWC with 45 μL mL^{-1} 1 M TEA buffer pH 10 and 300 mM (*R*)-**3** solved in CPME were tested with concentrations of 1−5 M **5**. The reactions were incubated at 30 °C and 1000 rpm. The same experimental setup was also applied for 30 mg mL^{-1} *Lb*ADH LWC; only the buffer amount was altered to 15 μL mL^{-1} 1 M TEA buffer pH 10. Samples were analyzed by gas chromatography (GC).

DOI: 10.1021/acssuschemeng.8b02107
ACS Sustainable Chem. Eng. 2018, 6, 11819−11826

Downstream Sequence and Product Purification by Crystallization. To determine the most suitable crystallization process, thermodynamic equilibria were evaluated. For primary studies, the complex mixture of the MARS was reduced to its key components: the solvent CPME, **3** (liquid above 25 °C), **4**, and **5**. Solubility data for **3** and **4** were determined separately in pure CPME and in the pure alcohol **5** at temperatures between 30 and 50 °C.

Investigations were carried out by solvent titration (CPME and **5**) at a controlled temperature (water bath) on a VWR VMS-C10 (VWR International, Radnor, PA, USA) equipped with a PT100 element, obtaining solubility areas for the solutes.[43] Solutes **3** and **4** were recovered as solids from CPME by slow evaporation at room temperature prior to reuse in subsequent experiments. Based on these experimental solubility data, which were converted to molar fractions (x [$\mathrm{mol_{compound\,\mathit{i}}\ mol^{-1}_{all\ compounds}}$]), the enthalpy of fusion (ΔH_f [kJ $\mathrm{mol^{-1}}$]) and the melting temperature (T_m [K]) were calculated for the solutes at various experimental temperatures (T [K]) by applying the simplified Schröder–van Laar equation (eq 1; R, gas constant).[43]

$$\ln(x(T)) = \frac{\Delta H_f}{R}\left(\frac{1}{T_m} - \frac{1}{T}\right) \quad (1)$$

For conversion to molar fractions, density data for **5** was taken from the GESTIS Substance Database (11.5.2017) at 25 °C, and for CPME at 20 °C.[44] With the Schröder–van Laar-based substance properties of **3** and **4** (ΔH_f and T_m), the solubilities were calculated using COSMOtherm version X17 (COSMOlogic GmbH & Co. KG, Leverkusen, Germany) in TZVP (triple valence plus polarization function) mode for the quaternary system.[45,46] Based on the experimentally determined solubilities and the calculated data, a downstream sequence was developed. First, a freeze crystallization of **5** was carried out at −30 °C in a 1 L triple-wall reactor type ATAV (HWS Labortechnik, Mainz, Germany), tempered by a Julabo Presto A40 (Julabo GmbH, Seelbach, Germany) and equipped with the thermal bath fluid HL60 (Julabo GmbH, Seelbach, Germany) as the tempering medium. Solid–liquid separation was performed by a suction filter using filter paper circles (ref no. 300009, Schleicher & Schüll, Düren, Germany), where the temperature was uncontrolled. Six fast filtration steps were performed to prevent the dissolution of **5**. In the second step, vacuum evaporation of CPME and **5** between 50 and 100 °C, and final cooling crystallization of **4** (T = 25 °C, cooling rate 0.15 °C $\mathrm{min^{-1}}$) were carried out in a 350 mL triple-wall reactor tempered by a Julabo CF31 (Julabo GmbH, Seelbach, Germany) and equipped with the thermal bath fluid H10 (Julabo GmbH, Seelbach, Germany) as the tempering medium. For vacuum evaporation, the vacuum pump VWR VP 10 Autovac (p < 10 mbar; VWR International, Radnor, PA, USA) with controlled distillate stream was utilized. The separation of the product crystals was first performed by centrifugation at 4000 rpm for 25 min with a Hettich Rotanta 460R (Andreas Hettich GmbH & Co. KG, Tuttlingen, Germany), and final washing was also performed on a suction filter.

Analytics. *NMR Spectra.* ^{1}H NMR spectra were recorded on a Bruker Avance DRX 600 MHz (Bruker, Billerica, MA, USA). The obtained ^{1}H NMR spectroscopic data were consistent with those in the literature (see Supporting Information (SI)).[10,47] Chiral HPLC analytics were conducted on a Dionex P680 HPLC System (Thermo Fisher Scientific, Waltham, MA, USA). GC analysis was performed on an Agilent 6890N GC system (Agilent, Glostrup Kommune, Denmark). Chiral GC analysis was also used to determine the crystal purity and stereoselectivity of the final product.

Chiral HPLC. Samples were analyzed on a Chiralpak IC (Diacel Corp., Germany) column (4.6 mm × 250 mm, 5 μm) under isocratic conditions of 30% isopropanol and 70% n-heptane at 1.5 mL $\mathrm{min^{-1}}$ flow rate and 20 °C. Toluene was applied as an internal standard. Elution times in order of peak appearance were as follows: toluene (210 nm) 2.3 min, **1** (275 nm) 4.8 min, (*R*)-**3** (275 nm) 5.4 min, (*S*)-**3** (275 nm) 6.3 min, (*R*)-2-hydroxy-1(4-(hydroxymethyl)-2-(4-methoxyphenyl)ethan-1-one (275 nm) 10.0 min, and (*S*)-2-hydroxy-1(4-(hydroxymethyl)-2-(4-methoxyphenyl)ethan-1-one (275 nm) 11.0 min. The total run time was 13 min.

Chiral GC. Samples were separated on a CP-Chirasil-Dex CB (Agilent J&W) column (i.d. 0.25 mm; 25 m × 0.25 μm). The furnace temperature was continuously increased from 50 to 190 °C over 25 min. The temperature was kept at a constant for 10 min; the total run time was 34 min. Elution times in order of peak appearance were as follows: **1** 16.7 min, dodecanol 19.8 min, 4-methoxy-benzaldehyde, (*R*)-**3** 22.2 min, (*S*)-**3** 22.5 min, (1*R*,2*R*)-**4** 25.8 min, (1*R*,2*S*)-**4** 26.2 min, (1*S*,2*R*)-**4** 26.4 min, and (1*S*,2*S*)-**4** after 26.8 min.

RESULTS AND DISCUSSION

The assembly of lipophobic biocatalysts in an artificial cascade requires prior reaction environment conditioning followed by individual step optimization to produce **4** in an organic reaction environment. MARS reaction environment conditioning is predominantly manipulated by solvent selection. In this study, ethers displayed a high biocatalysis-promoting capability. CPME was seen as a particularly promising choice for a MARS setup, as it enabled the highest catalytic activity (see SI, Figure S1). In addition, its safety and eco-friendly characteristics led to a general reaction environment conditioning based on CPME.[35,44]

Fed-Batch Design Overcomes Substrate Inhibition. In batch, high STYs are dependent on high substrate concentrations. Starting concentrations of the first step were thus increased until substrate inhibition occurred. This revealed 500 mM 4-methoxy-benzaldehyde (**1**) to be optimal (data not provided). Higher concentration led to biocatalyst inhibition. In contrast, acetaldehyde (**2**) was only applicable until 175 mM for *Pf*BAL and 100 mM for *Pp*BFD varL461A (see SI, Figure S2). Higher concentrations resulted in rapid activity decline. Interestingly, both carboligases sustained higher concentrations of acetaldehyde in aqueous conditions, as reported by others.[22,48] The reason for the increased sensitivity in MARS is currently not known. Unfortunately, a high yield of **3** requires an excess of **2**.[22,49]

Substrate **2** was therefore pulsed in a simple *fed*-batch mode. The pulse intervals were empirically optimized to a maximum yield of **3** (see SI, Figures S3–S5). This enabled an 80% yield (400 mM) of the intermediate (*R*)-**3** within 2 h and 99% *enantiomeric excess* (*ee*) with *Pf*BAL. Notably, with *Pp*BFD varL461A a yield of 56% (280 mM) (*S*)-**3** with 99% *ee* within 3 h was achieved. In contrast, the wild-type enzyme *Pp*BFD wt reportedly yields only 23% (*S*)-**3** with an ee of 92%, thus confirming the catalyst selection.[50] Others investigated the same enzymes in a cascade with 500 mM unsubstituted aromatic substrate in a different MARS setup.[15,16] There, an 80% yield of the respective (*R*)-derivative was obtained in 2 h and 76% yield of the respective (*S*)-derivative was obtained in 6 h.[15,16] These and our findings thus suggest that MARS is a robust system for obtaining high STYs and excellent ee's in an organic environment with otherwise solvent-sensitive biocatalysts.

NADPH Regeneration with Smart Cosubstrates and Self-Sufficient Cascade Design. In the individual second step optimization, two stereocomplementary NADPH-dependent alcohol dehydrogenases, RADH and *Lb*ADH, were investigated in their reductive potential of (*R*)-**3**. NADPH is endogenously provided by the applied LWCs. However, its obligatory regeneration challenges atom economy and *E*-factors in processes. Therefore, two nicotinamide regeneration options were investigated in a single-step experiment to determine their applicability: (i) a parallel cascade with a smart

DOI: 10.1021/acssuschemeng.8b02107
ACS Sustainable Chem. Eng. 2018, 6, 11819–11826

Table 1. Comparison of Process Parameters for the Production of All Four Stereoisomers of 4-Methoxyphenyl-1,2-propanediol in Sequential and Simultaneous Modes: End Point Detection

	sequential mode[g]						simultaneous mode[l]					
product isomer	conv[a] [%]	c_{end}[b] [g L^{-1}]	STY[c] [g L^{-1} day^{-1}]	*ee*[d] [%]	*de*[e] [%]	*E*-factor[f]	conv[a] [%]	c_{end}[b] [g L^{-1}]	STY[c] [g L^{-1} day^{-1}]	*ee*[d] [%]	*de*[e] [%]	*E*-factor[f]
(1*R*,2*R*)[h]	71.2	60.1	165 (10 h)	99	99	13.8	77.5	62.7	109 (10 h)	99	99	12.3
(1*R*,2*S*)[i]	37.2	33.9	41.4 (10 h)	99	99	21.4	0.2	0.3	0.6 (7 h)	99	99	n.a.
(1*S*,2*R*)[j]	41.7	37.4	84.4 (9 h)	99	99	24.3	2.5	4.6	7.0 (10 h)	99	99	n.a.
(1*S*,2*S*)[k]	19.2	17.47	18.1 (9 h)	99	99	45.6	0.1	0.1	0.6 (7 h)	99	99	n.a.

[a]4-Methoxy-benzaldehyde conversion (conv) to 4-methoxyphenyl-1,2-propanediol (see SI, Table S1, for conversion of each cascade step). [b]Final product titer (c_{end}) was calculated from the final reaction solution after 24 h. [c]Space-time yield (STY). [d]Enantiomeric excess (*ee*). [e]Diastereomeric excess (*de*). [f]The *E*-factor accounts for all required substrates, catalysts, and solvents in the reaction. n.a. = not applicable. Calculation, see SI, eq S2. [g]Reaction conditions include reaction volume 4 mL. [h](1*R*,2*R*)-Anethole-diol production: 25 mg mL^{-1} *P. fluorescens* benzaldehyde lyase (BAL) with 25 μL mL^{-1} 1 M TEA buffer pH 10, 30 mg mL^{-1} *Ralstonia* sp. alcohol dehydrogenase (RADH) with 45 μL mL^{-1} 1 M TEA buffer pH 10, 500 mM 4-methoxy-benzaldehyde, 180 mM acetaldehyde, 3 M 4-methoxybenzyl alcohol. [i](1*R*,2*S*)-Anethole-diol production: 25 mg mL^{-1} BAL with 25 μL mL^{-1} 1 M TEA buffer pH 10, 90 mg mL^{-1} *L. brevis* alcohol dehydrogenase (*Lb*ADH) with 60 μL mL^{-1} 1 M TEA buffer pH 10, 500 mM 4-methoxy-benzaldehyde, 180 mM acetaldehyde, 5 M 4-methoxybenzyl alcohol. [j](1*S*,2*R*)-Anethole-diol production: 100 mg mL^{-1} *P. putida* benzoylformate decarboxylase variant L461A (BFD) with 100 μL mL^{-1} 1 M TEA buffer pH 10, 30 mg mL^{-1} RADH with 45 μL mL^{-1} 1 M TEA buffer pH 10, 500 mM 4-methoxy-benzaldehyde, 120 mM acetaldehyde, 3 M 4-methoxybenzyl alcohol. [k](1*S*,2*S*)-Anethole-diol production: 100 mg mL^{-1} BFD with 100 μL mL^{-1} 1 M TEA buffer pH 10, 90 mg mL^{-1} *Lb*ADH with 45 μL mL^{-1} 1 M TEA buffer pH 10, 500 mM 4-methoxy-benzaldehyde, 120 mM acetaldehyde, 5 M 4-methoxybenzyl alcohol. [l]The reactions are equal to sequential mode, with the exception that only 100 mM 4-methoxy-benzaldehyde was applied; all reactions were pulsed with acetaldehyde to total amounts of 650 mM; total reaction volume 1 mL; 30 °C and 1000 rpm; *n* = 3.

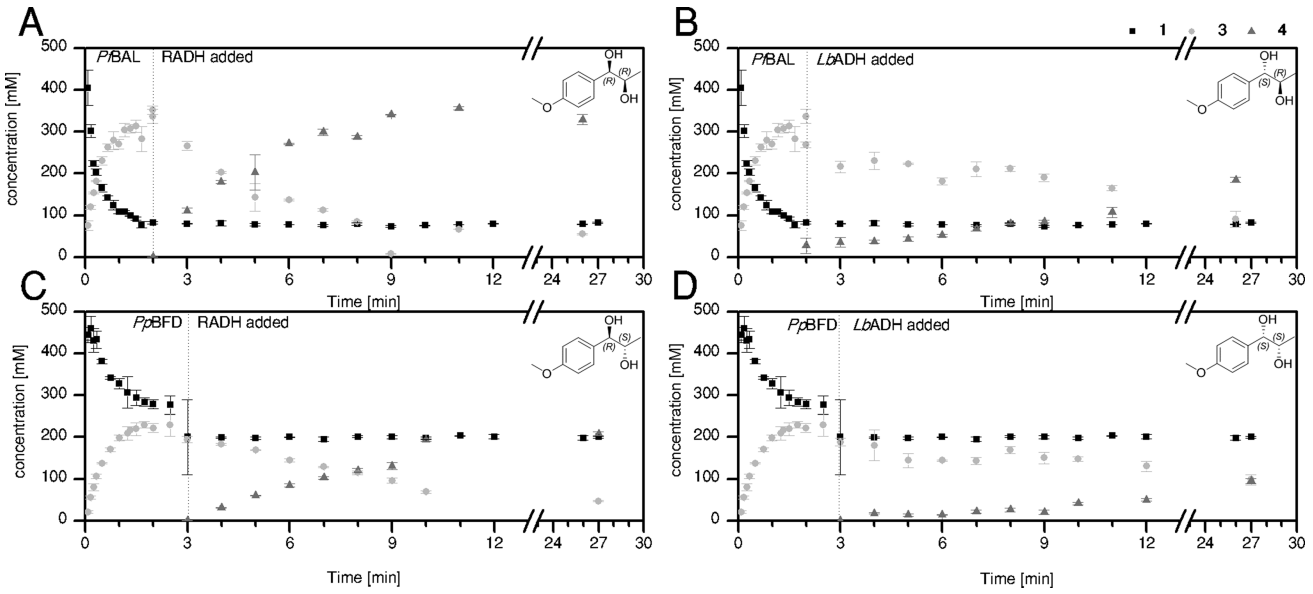

Figure 3. Sequential cascade mode for all stereoisomers of 4-methoxyphenyl-1,2-propanediol (A–D). Once carboligation has reached its maximum conversion, the alcohol dehydrogenase and cosubstrate are added, and the second step takes place. First step: 25 mg mL^{-1} *P. fluorescens* benzaldehyde lyase (*Pf*BAL) lyophilized whole cells (LWC) were incubated with 500 mM 4-methoxy-benzaldehyde and 180 mM acetaldehyde in cyclopentyl methyl ether (CPME) with 25 μL mL^{-1} 1 M TEA buffer pH 10 (A, B). 90 mM acetaldehyde was dosed after 5, 12, 20, 30, 45, and 60 min; 100 mg mL^{-1} *P. putida* benzoylformate decarboxylase (*Pp*BFD varL461A) variant L461A LWC was incubated with 500 mM 4-methoxy-benzaldehyde and 120 mM acetaldehyde in CPME with 100 μL mL^{-1} 1 M TEA buffer pH 10 (C, D). 90 mM acetaldehyde was pulsed after 10, 20, 30, 45, 60, 75, 90, and 105 min. Second step: 30 mg mL^{-1} *Ralstonia* sp. alcohol dehydrogenase (RADH) LWC was added to the reaction solution with 45 μL mL^{-1} 1 M TEA buffer pH 10 and 3 M 4-methoxybenzyl alcohol (A, C). 90 mg mL^{-1} *L. brevis* ADH (*Lb*ADH) LWC was added with 60 μL mL^{-1} 1 M TEA buffer pH 10 and 5 M 4-methoxybenzyl alcohol to the reaction solution (B, D). 30 °C, 1000 rpm; HPLC and GC analysis; *n* = 3.

cosubstrate and (ii) a cosubstrate that allows the setup of a self-sufficient cascade (Figure 2).[42,51−53]

In a self-sufficient cascade, the coproduct formed is recyclable in the first step of the cascade (Figure 2). Here, only 4-methoxybenzyl alcohol (**5**) was investigated, since ethanol is not within the substrate scope of RADH.[23] Besides recycling the oxidation product of **5**, smart cosubstrates were investigated. Since smart cosubstrates possess two hydroxyl groups for oxidation, 0.5 M 1,5-pentanediol, 1,4-pentanediol, and 3-methyl-1,5-pentanediol were compared against each other and 1 M self-sufficient cosubstrate **5**. Within this comparison, RADH yielded 85% product with the cosubstrates 1,4-pentanediol, 3-methyl-1,5-pentanediol, and **5** (see SI, Figure S6). *Lb*ADH achieved a maximum conversion of 25% with 1,5-pentanediol after 24 h. These results reflect the different substrate scopes and activities of *Lb*ADH and

DOI: 10.1021/acssuschemeng.8b02107
ACS Sustainable Chem. Eng. 2018, 6, 11819−11826

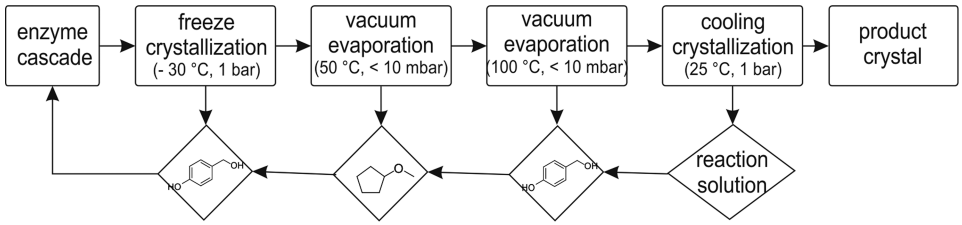

Figure 4. Block flow diagram of downstream product crystallization.

RADH.[23,26] Combined, these results favor smart cosubstrates, since their application renders cosubstrate excess almost obsolete. Unfortunately, in the subsequent downstream purification, slight thermal conditioning at 35 °C already resulted in the untargeted polymerization of the lactone with the desired diol product **4**, which rendered product isolation impossible.

The self-sufficient cascade design with **5** was thus selected, as it permits product isolation and features excellent atom economies of 99.9% in simultaneous cascade mode as will be presented in the section Cascade Operation in Sequential and Simultaneous Mode To Obtain All Product Isomers.[54] Different concentrations of **5** as a cosubstrate were examined, revealing a 6-fold excess as optimal for RADH to achieve 90% conversion of 400 mM **3** within 6 h. *Lb*ADH required a 10-fold excess, in which the solvent is completely subsisted by the cosubstrate, to drive the reaction to a conversion of 38% within 24 h (see SI, Figure S7). The required cosubstrate surplus is reconcilable due to a selective product isolation.

Cascade Operation in Sequential and Simultaneous Mode To Obtain All Product Isomers. The optimized carboligation and the self-sufficient reductive step were assembled to a cascade in one-pot, which was tested in simultaneous and sequential cascade modes. In simultaneous mode, all catalysts and substrates were present from the start and the reaction progressed directly to the product. In sequential mode, the substrates and catalyst of the first step were present from the beginning. When the intermediate concentration peaked, the cosubstrate and the catalyst of the second step were added. In comparison, the sequential mode achieved superior STYs of up to 165 g L^{-1} day^{-1} and *E*-factors ranging between 13 and 45 for all four product isomers (Table 1; *E*-factors see SI, Tables S2 and S3 and eq S2).[54−56] Here, with *Pf*BAL higher conversions were observed than with *Pp*BFD varL461A. This finding has also been observed elsewhere.[15,57] In the second step, the highly aromatic substrate-affine RADH outperforms *Lb*ADH, which prefers smaller substrates.[23,26] It was thus anticipated that (1*R*,2*R*)-**4** would achieve the highest STY, as verified by the obtained results. Nevertheless, all four isomers were obtained with excellent to satisfying STYs (Figure 3).

In simultaneous mode, only the (1*R*,2*R*)-**4** isomer was obtained with STY > 109 g L^{-1} day^{-1} and an *E*-factor of 12. Here, substrate cross-reactivity averts the synthesis of the other three product isomers. *Lb*ADH exhibits a higher affinity toward the aliphatic substrate **2** than to the aromatic intermediate **3**, thus depriving the cascade of substrate.[15] This affects the final yields of (1*S*,2*R*)-**4** and (1*S*,2*S*)-**4** negatively. In contrast, RADH prefers an aromatic substrate, such as aldehyde **1**, alcohol **5**, and intermediate **3**.[23] Theoretically, RADH could also interfere in the first cascade step by reducing the aromatic aldehyde **1** to the corresponding alcohol **5**. However, in terms of thermodynamics, the excess of **5** in the reaction prevented this. Further, *Pp*BFD varL461A introduces no cross-reactivity, but suffers an observable sensitivity toward the presence of elevated alcohol concentrations. Similar observations have been reported for the wild-type enzyme.[15,58] Therefore, only the combination of *Pf*BAL and RADH permits a successful synthesis of (1*R*,2*R*)-**4** in simultaneous mode (see SI, Figure S8).

In conclusion, the sequential mode was found to be superior, since it allows higher STYs and grants access to all four product isomers. Notably, all four product isomers were obtained in optimal stereoselectivity with *ee*'s and *diastereomeric excesses* (*de*'s) of >99%, proving the high selectivity of selected catalysts. Furthermore, all four isomers were synthesized with satisfying *E*-factors well within the range of industrially defined benchmarks of 5 to >50 for fine chemicals and even excellent *E*-factors for pharmaceuticals (25 to >100).[55,56] In the future, catalyst engineering or new catalyst discovery might reduce cross-reactivity and sensitivity, which would enable a simultaneous mode for all product isomers.

Preparative-Scale Production of (1*R*,2*R*)-4 Including Product Crystallization. Due to its superior STY and its access to all four product isomers, the sequential synthesis of (1*R*,2*R*)-**4** was scaled up to a production volume of 0.5 L. The product was then isolated at defined parameters by crystallization.

Remarkably, the sequential cascade mode for the upstream synthesis of (1*R*,2*R*)-**4** proved to be directly scalable from 4 to 500 mL, with a final product concentration of 75 g L^{-1} and excellent stereoselectivity of *ee* and *de* values of >99% in the larger volume (see Figure S9). Furthermore, the STY in preparative scale corresponded with results obtained from 1 mL scale, with a satisfying 148 g L^{-1} day^{-1} and an overall conversion of 82%.

Prior to consecutive downstream purification, different compound behavior was investigated in the reaction solution. The obtained results enabled a model-based prediction of suitable crystallization parameters for the product (see SI, Figure S11). These simulations in COSMOthermX17 revealed an enrichment of the product diol **4** to be necessary in achieving a supersaturation of the 1,2-diol. The concentration of **4** required to achieve supersaturation depends on the ratio of the solvent/cosubstrate mixture in the mother liquor. For this reason, both amounts of CPME and cosubstrate **5** need to be reduced. Therefore, a downstream process was devised consisting of (i) a freeze crystallization to remove the cosubstrate **5**, followed by (ii) a vacuum evaporation of CPME (Figure 4).

First, the reduction of the cosubstrate **5** was successfully targeted by utilizing the high melting point of the substance (T_m = 23 °C) in a freeze crystallization at −30 °C. The crystals obtained had a purity of 55.5% (w w^{-1}) of the cosubstrate **5**. The main side component was CPME (37.6% (w w^{-1})), in addition to small amounts of the product **4** (5.7% (w w^{-1}))

DOI: 10.1021/acssuschemeng.8b02107
ACS Sustainable Chem. Eng. 2018, 6, 11819−11826

and intermediate **3** (1.2% (w w^{-1})). In total, 2.4% (w w^{-1}) of **5** was removed (Figure 5, process steps 2 and 3). The overlying solid−liquid equilibrium of **5** in CPME complicates its efficient separation.

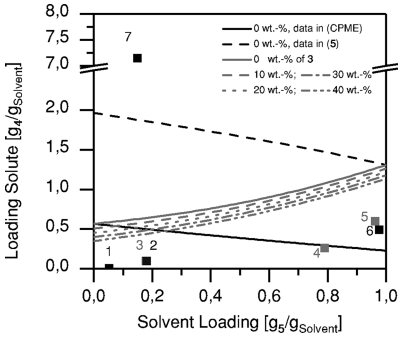

Figure 5. Simulated solubility data of **4** in product solution and experimental concentrations of **4** along different downstream process steps. Depicted is the simulated solid−liquid equilibrium of **4** with CPME and **5** for different percentages (w w^{-1}) of **3** in solution at 25 °C. The symbols depict experimental compositions in solution after processing steps in the downstream sequence: 1, feed to enzyme cascade; 2, product of enzyme cascade; 3, first crystallization of **5**; 4, after evaporation at 50 °C and attempted crystallization of **5**; 5, after evaporation at 100 °C; 6, mother liquor after cooling crystallization of **4** to 25 °C; 7, crystal-enriched phase after centrifugation. Identical experimental and calculated data were also obtained for the intermediate **3** (see SI, Figure S12).

Vacuum evaporation at 50 °C was then applied, mainly to remove CPME and the remaining substrates **1** and **2** (Figure 5, process steps 3 and 4). This again led to an accumulation of the product diol **4**, predominantly in cosubstrate **5**, and smaller amounts of CPME. The simulation demonstrates that an increased amount of **5** in a solvent mixture of **5** and CPME is unfavorable for product crystallization. Instead, vacuum evaporation at 100 °C removed sufficient amounts of **5** to achieve supersaturation. Selective crystal formation of the desired product **4** formed during a subsequent cooling crystallization to 25 °C (Figure 5, process steps 4 and 5).

When the experimentally determined product concentration of each step is aligned with the simulated solubility range of **4** at different conditions with COSMOthermX17 (Figure 5), it becomes apparent that no crystallization should be expected during the final evaporation and cooling crystallization step. Although this represents a deviation between experimental results and simulation, it is still well within the expected range of error discussed for COSMOtherm calculations.[44] The cause of this deviation is the limited capability of COSMOthermX17 to project the real solvent mixture conditions. Here, the program relies on experimental solubility in pure CPME and in pure **5**. The precision of the simulated product solubility was improved by calculating the binary interaction parameters from the experimental product concentration of the mother liquor after final crystallization. Nevertheless, the approximation by COSMOthermX17 is well-suited to generating a first impression of the behavior in the quaternary system comprising the product **4**, the intermediate **3**, the cosubstrate **5**, and the solvent CPME. Thus COSMO simulations are still valuable to reduce experimental effort and isolation costs.

Ultimately, crystals were isolated by centrifugation in a grayish bottom phase, which was separated from the top solution (Figure 5 process steps 5−7). Crystals with a purity of >99% of **4** were obtained after washing with cooled acetone. No side components were detected.

Advantageously, the efficient product crystallization permits a direct recycling of the remaining substrates, cosubstrate, intermediate, and CPME for the next batch. This remarkably reduces *E*-factors of the overall process close to 1 (see SI, Tables S2 and S3). However, it must be noted that the current downstream purification does not isolate **5** efficiently enough from other compounds to avoid a potential inhibition of *Pp*BFD varL461A during reapplication.

In conclusion, the sequential cascade was directly scaled up from 4 to 500 mL, achieving the same STY as well as product concentration and stereoselectivities. In the consecutive downstream processing, an isolated yield of 38% with a crystal purity of >99% was obtained. In future, downstream process efficiency could be increased by optimizing the separation of **5** by freeze crystallization. This would have a positive impact on operation parameters, such as seeding and washing strategies, to simplify a subsequent solid−liquid separation of crystals and ultimately increase isolated yields. It would also enable an isolated recovery of each reaction compound and thus facilitate direct recyclability for all four product isomer cascades.

CONCLUSION

In this study, we demonstrated the impact of a sophisticated overall process design guided by *E*-factors and STY considerations. Four stereocomplementary biocatalytic cascades were successfully assembled for the sustainable synthesis of all four stereoisomers of 4-methoxyphenyl-1,2-propanediol with excellent *ee* and *de* values of >99%. Clever coproduct recycling enables a self-sufficient cascade design with an atom economy of 57% in sequential mode and 99% in simultaneous mode. All product isomers can be gained effectively in sequential operation mode. A simultaneous operation is restricted to the (1*R*,2*R*)-**4** product isomer due to cross-reactivities. Space-time yields of up to 165 g L^{-1} day^{-1} are achieved in the applied hydrophobic microaqueous reaction system based on CPME. Furthermore, the linear transferability to a large scale was exemplarily demonstrated on (1*R*,2*R*)-**4** with a final product conversion of 82% and >99% *de* and *ee* in a 0.5 L scale. During subsequent downstream purification, the product was successfully crystallized with an isolated yield of 38% and a purity of >99%. Notably, this would enable the potential reapplication of all substrates, cosubstrates, and the solvent in a next batch, which reduces the *E*-factor of the whole process to potentially 1. Overall, the process aligns neatly with other biocatalytic syntheses for 1,2-diols, thus highlighting the significant potential of biocatalysis to synthesize a whole derivative product platform in a hydrophobic environment.

In the future, the current process efficiency could be increased both upstream and downstream. Upstream, precise reaction kinetics including inhibition constants would permit a refined *fed*-batch process of the first catalytic step. A simultaneous cascade mode for all stereoisomers might be enabled by enzyme engineering or the discovery of novel substrate sensitive catalysts with no cross-reactivity. Downstream, a more efficient freeze crystallization separation of the alcohol **5** might speed up the crystallization process and facilitate crystal separation.

DOI: 10.1021/acssuschemeng.8b02107
ACS Sustainable Chem. Eng. 2018, 6, 11819−11826

■ ASSOCIATED CONTENT

Supporting Information

The Supporting Information is available free of charge on the ACS Publications website at DOI: 10.1021/acssuschemeng.8b02107.

Genetic information of applied catalysts, initial activity measurements; empiric conditioning of MARS, optimal acetaldehyde starting condition, acetaldehyde pulsing optimization for fed batch, evaluation of optimal cosubstrate concentrations for the reductive step, cascade operation mode, preparative scale for (1*R*,2*R*)-**4** synthesis, equations to calculate atom efficiency and *E*-factors, vapor−liquid equilibria of CPME and **5** in COSMOthermX1, product crystallization modeling for efficient downstream processing, simulated solubility of the intermediate, product crystal pictures, ^{1}H NMR spectra (PDF)

■ AUTHOR INFORMATION

Corresponding Author

*E-mail: do.rother@fz-juelich.de. Tel.: +49 2461 61-6772. Fax: +49 2461 61-3870.

ORCID

Reinhard Oeggl: 0000-0003-1189-3142

Author Contributions

‖R.O. and T.M. contributed equally to this work. All authors contributed to the manuscript. R.O. and D.R. designed the cascade, while T.M. and A.J. designed the crystallization process. Experimental procedures were performed by R.O. and T.M. The experimental procedures were supervised by R.O., T.M., A.J. and D.R. R.O., T.M., A.J., and D.R. helped finalize the manuscript. All authors have approved the final version of the manuscript.

Notes

The authors declare no competing financial interest.

■ ACKNOWLEDGMENTS

We would like to thank the Helmholtz Association for funding this project within the framework of the young investigators' group "synthetic enzyme cascades". We would also like to thank our technicians Doris Hahn and Ursula Mackfeld.

■ ABBREVIATIONS

*Pf*BAL = *Pseudomonas fluorescens* benzaldehyde lyase
*Pp*BFD = *Pseudomonas putida* benzoylformate decarboxylase
CPME = cyclopentyl methyl ether
E. coli = *Escherichia coli*
E-factor = environmental factor [1]
ΔH_f = heat of fusion, melting enthalpy [kJ mol^{-1}]
*Lb*ADH = *Lactobacillus brevis* alcohol dehydrogenase
LWC = lyophilized whole cells
R = gas constant [J K^{-1} mol^{-1}]
n.a. = not applicable
RADH = *Ralstonia* sp. alcohol dehydrogenase
STY = space-time yield [g L^{-1} day^{-1}]
T_m = melting temperature [K]
T = process temperature [K]
TZVP = triple valence plus polarization function
x = molar fraction [$mol_{compound\ i}$ $mol^{-1}_{all\ compounds}$]

■ REFERENCES

(1) Sheldon, R. A.; Woodley, J. M. Role of Biocatalysis in Sustainable Chemistry. *Chem. Rev.* **2018**, *118* (2), 801−838.
(2) Song, D.-K.; Son, J.-K. Novel therapeutical use of erythro-1(4-methoxyphenyl)-1,2-propanediol. WIPO 03/084522 A1, 2003.
(3) Lee, S. W.; Li, G.; Lee, K. S.; Jung, J. S.; Xu, M. L.; Seo, C. S.; Chang, H. W.; Kim, S. K.; Song, D. K.; Son, J. K. Preventive agents against sepsis and new phenylpropanoid glucosides from the fruits of *Illicium verum*. *Planta Med.* **2003**, *69* (9), 861−864.
(4) Freire, R. S.; Morais, S. M.; Catunda-Junior, F. E. A.; Pinheiro, D. C. S. N. Synthesis and antioxidant, anti-inflammatory and gastroprotector activities of anethole and related compounds. *Bioorg. Med. Chem.* **2005**, *13* (13), 4353−4358.
(5) Ohta, H.; Ozaki, K.; Konishi, J.; Tsuchihashi, G. Reductive C2-homologation of substituted benzaldehydes by fermenting baker's yeast. *Agric. Biol. Chem.* **1986**, *50* (5), 1261−1266.
(6) Acetti, D.; Brenna, E.; Fuganti, C. A new enzymatic approach to (*R*)-tamsulosin hydrochloride. *Tetrahedron: Asymmetry* **2007**, *18* (4), 488−492.
(7) Cheung, C. W. Y.; Gibbons, N.; Johnson, D. W.; Nicol, D. L. Silibinin - a promising new teatment for cancer. *Anti-Cancer Agents Med. Chem.* **2010**, *10* (3), 186−195.
(8) Sharpless, K. B.; Amberg, W.; Bennani, Y. L.; Crispino, G. A.; Hartung, J.; Jeong, K. S.; Kwong, H. L.; Morikawa, K.; Wang, Z. M.; Xu, D. Q.; et al. The osmium-catalyzed asymmetric dihydroxylation - a new ligand class and a process improvement. *J. Org. Chem.* **1992**, *57* (10), 2768−2771.
(9) Griffith, J. C.; Jones, K. M.; Picon, S.; Rawling, M. J.; Kariuki, B. M.; Campbell, M.; Tomkinson, N. C. O. Alkene *syn* dihydroxylation with malonoyl peroxides. *J. Am. Chem. Soc.* **2010**, *132* (41), 14409−14411.
(10) Kulig, J.; Simon, R. C.; Rose, C. A.; Husain, S. M.; Häckh, M.; Lüdeke, S.; Zeitler, K.; Kroutil, W.; Pohl, M.; Rother, D. Stereoselective synthesis of bulky 1,2-diols with alcohol dehydrogenases. *Catal. Sci. Technol.* **2012**, *2* (8), 1580.
(11) Mohan, R. S.; Gavardinas, K.; Kyere, S.; Whalen, D. L. Spontaneous hydrolysis reactions of *cis*- and *trans*-*β*-methyl-4-methoxystyrene oxides (anethole oxides): Buildup of trans-anethole oxide as an intermediate in the spontaneous reaction of *cis*-anethole oxide. *J. Org. Chem.* **2000**, *65* (5), 1407−1413.
(12) Ashikari, Y.; Nokami, T.; Yoshida, J. I. Oxidative hydroxylation mediated by alkoxysulfonium ions. *Org. Lett.* **2012**, *14* (3), 938−941.
(13) Notz, W.; List, B. Catalytic asymmetric synthesis of anti-1,2-diols. *J. Am. Chem. Soc.* **2000**, *122* (30), 7386−7387.
(14) Torres, C. C.; Campos, C. H.; Fierro, J. L. G.; Reyes, P.; Ruiz, D. Journal of Molecular Catalysis A : Chemical Enantioselective hydrogenation of 1-phenyl-1,2-propanodione on cinchonidine-modified Rh/MCM-41 catalysts. *J. Mol. Catal. A: Chem.* **2014**, *392*, 321−328.
(15) Wachtmeister, J.; Jakoblinnert, A.; Rother, D. Stereoselective two-step biocatalysis in organic solvent: Toward all stereoisomers of a 1,2-diol at high product concentrations. *Org. Process Res. Dev.* **2016**, *20* (10), 1744−1753.
(16) Jakoblinnert, A.; Rother, D. A two-step biocatalytic cascade in micro-aqueous medium: using whole cells to obtain high concentrations of a vicinal diol. *Green Chem.* **2014**, *16* (7), 3472−3482.
(17) Kihumbu, D.; Stillger, T.; Hummel, W.; Liese, A. Enzymatic synthesis of all stereoisomers of 1-phenylpropane-1,2-diol. *Tetrahedron: Asymmetry* **2002**, *13* (10), 1069−1072.
(18) Iding, H.; Dünnwald, T.; Greiner, L.; Liese, A.; Müller, M.; Siegert, P.; Grötzinger, J.; Demir, A. S.; Pohl, M. Benzoylformate decarboxylase from *Pseudomonas putida* as stable catalyst for the synthesis of chiral 2-hydroxy ketones. *Chem. - Eur. J.* **2000**, *6* (8), 1483−1495.
(19) Gocke, D.; Walter, L.; Gauchenova, E.; Kolter, G.; Knoll, M.; Berthold, C. L.; Schneider, G.; Pleiss, J.; Müller, M.; Pohl, M. Rational protein design of ThDP-dependent enzymes - Engineering stereoselectivity. *ChemBioChem* **2008**, *9* (3), 406−412.

DOI: 10.1021/acssuschemeng.8b02107
ACS Sustainable Chem. Eng. 2018, 6, 11819−11826

(20) Demir, A. S.; Ayhan, P.; Sopaci, S. B. Thiamine pyrophosphate dependent enzyme catalyzed reactions: Stereoselective C-C bond formations in water. *Clean: Soil, Air, Water* **2007**, *35* (5), 406−412.
(21) González, B.; Vicuña, R. Benzaldehyde lyase, a novel thiamine PPi-requiring enzyme, from *Pseudomonas fluorescens* Biovar I. *J. Bacteriol.* **1989**, *171* (5), 2401−2405.
(22) Domingeuz de María, P.; Stillger, T.; Pohl, M.; Kiesel, M.; Liese, A.; Gröger, H.; Trauthwein, H. Enantioselective C-C bond ligation using recombinant *Escherichia coli* whole-cell biocatalysts. *Adv. Synth. Catal.* **2008**, *350* (1), 165−173.
(23) Kulig, J.; Frese, A.; Kroutil, W.; Pohl, M.; Rother, D. Biochemical characterization of an alcohol dehydrogenase from *Ralstonia* sp. *Biotechnol. Bioeng.* **2013**, *110* (7), 1838−1848.
(24) Lavandera, I.; Kern, A.; Ferreira-Silva, B.; Glieder, A.; de Wildeman, S.; Kroutil, W. Stereoselective bioreduction of bulky-bulky ketones by a novel ADH from *Ralstonia* sp. *J. Org. Chem.* **2008**, *73* (15), 6003−6005.
(25) Hoyos, P.; Sansottera, G.; Fernández, M.; Molinari, F.; Sinisterra, J. V.; Alcántara, A. R. Enantioselective monoreduction of different 1,2-diaryl-1,2-diketones catalysed by lyophilised whole cells from *Pichia glucozyma*. *Tetrahedron* **2008**, *64* (34), 7929−7936.
(26) Leuchs, S.; Greiner, L. Alcohol dehydrogenase from *Lactobacillus brevis*: A versatile robust catalyst for enantioselective transformations. *Chem. Biochem. Eng. Q.* **2011**, *25* (2), 267−281.
(27) Yamane, T. Importance of moisture content control for enzymatic reactions in organic solvents: A novel concept of 'microaqueous.'. *Biocatalysis* **1988**, *2* (1), 1−9.
(28) Jakoblinnert, A.; Mladenov, R.; Paul, A.; Sibilla, F.; Schwaneberg, U.; Ansorge-Schumacher, M. B.; Domingeuz de María, P. Asymmetric reduction of ketones with recombinant *E. coli* whole cells in neat substrates. *Chem. Commun.* **2011**, *47* (44), 12230.
(29) Lin, G.; Han, S.; Li, Z. Enzymatic synthesis of (*R*)-cyanohydrins by three (*R*)-oxynitrilase sources in micro-aqueous organic medium. *Tetrahedron* **1999**, *55* (12), 3531−3540.
(30) Hibino, A.; Ohtake, H. Use of hydrophobic bacterium *Rhodococcus rhodochrous* NBRC15564 expressed thermophilic alcohol dehydrogenases as whole-cell catalyst in solvent-free organic media. *Process Biochem.* **2013**, *48* (5−6), 838−843.
(31) de Gonzalo, G.; Lavandera, I.; Faber, K.; Kroutil, W. Enzymatic reduction of ketones in "micro-aqueous" media catalyzed by ADH-A from *Rhodococcus ruber*. *Org. Lett.* **2007**, *9* (11), 2163−2166.
(32) Doukyu, N.; Ogino, H. Organic solvent-tolerant enzymes. *Biochem. Eng. J.* **2010**, *48* (3), 270−282.
(33) Tufvesson, P.; Lima-Ramos, J.; Al Haque, N.; Gernaey, K. V.; Woodley, J. M. Advances in the Process Development of Biocatalytic Processes. *Org. Process Res. Dev.* **2013**, *17* (10), 1233−1238.
(34) Prat, D.; Hayler, J.; Wells, A. A survey of solvent selection guides. *Green Chem.* **2014**, *16* (10), 4546−4551.
(35) Prat, D.; Wells, A.; Hayler, J.; Sneddon, H.; McElroy, C. R.; Abou-Shehada, S.; Dunn, P. J. CHEM21 selection guide of classical- and less classical-solvents. *Green Chem.* **2016**, *18* (1), 288−296.
(36) Saeedi, A.; Omidi, M.; Khoshnoud, M. J.; Mohammadi-Bardbori, A. Exposure to methyl *tert*-butyl ether (MTBE) is associated with mitochondrial dysfunction in rat. *Xenobiotica* **2017**, *47* (5), 423−430.
(37) Roslev, P.; Lentz, T.; Hesselsoe, M. Microbial toxicity of methyl *tert*-butyl ether (MTBE) determined with fluorescent and luminescent bioassays. *Chemosphere* **2015**, *120*, 284−291.
(38) Faber, K. Introduction and Background Information. In *Biotransformations in Organic Chemistry*; Springer: Berlin, 2011; pp 1−30.
(39) Hummel, W.; Gröger, H. Strategies for regeneration of nicotinamide coenzymes emphasizing self-sufficient closed-loop recycling systems. *J. Biotechnol.* **2014**, *191*, 22−31.
(40) Schrittwieser, J. H.; Velikogne, S.; Hall, M.; Kroutil, W. Artificial biocatalytic linear cascades for preparation of organic molecules. *Chem. Rev.* **2018**, *118*, 270.
(41) Schmidt, S.; Scherkus, C.; Muschiol, J.; Menyes, U.; Winkler, T.; Hummel, W.; Gröger, H.; Liese, A.; Herz, H.; Bornscheuer, U. T. An enzyme cascade synthesis of ε-caprolactone and its oligomers. *Angew. Chem., Int. Ed.* **2015**, *54* (9), 2784−2787.
(42) Kara, S.; Spickermann, D.; Schrittwieser, J. H.; Leggewie, C.; van Berkel, W. J. H.; Arends, I. W. C. E.; Hollmann, F. More efficient redox biocatalysis by utilising 1,4-butanediol as a 'smart cosubstrate.'. *Green Chem.* **2013**, *15* (2), 330.
(43) Beckmann, W. Crystallization: Introduction. In *Crystallization*; Wiley-VCH Verlag GmbH & Co. KGaA: Weinheim, 2013; pp 1−5.
(44) Watanabe, K.; Yamagiwa, N.; Torisawa, Y. Cyclopentyl methyl ether as a new and alternative process solvent. *Org. Process Res. Dev.* **2007**, *11* (2), 251−258.
(45) Eckert, F.; Klamt, A. Fast solvent screening via quantum chemistry: COSMO-RS approach. *AIChE J.* **2002**, *48* (2), 369−385.
(46) Abramov, Y. A.; Loschen, C.; Klamt, A. Rational coformer or solvent selection for pharmaceutical cocrystallization or desolvation. *J. Pharm. Sci.* **2012**, *101* (10), 3687−3697.
(47) Sy, L. K.; Brown, G. D. Novel phenylpropanoids and lignans from *Illicium verum*. *J. Nat. Prod.* **1998**, *61* (8), 987−992.
(48) Franken, B.; Eggert, T.; Jaeger, K. E.; Pohl, M. Mechanism of acetaldehyde-induced deactivation of microbial lipases. *BMC Biochem.* **2011**, *12* (1), 10.
(49) Domingeuz de María, P.; Stillger, T.; Pohl, M.; Wallert, S.; Drauz, K.; Gröger, H.; Trauthwein, H.; Liese, A. Preparative enantioselective synthesis of benzoins and (*R*)-2-hydroxy-1-phenyl-propanone using benzaldehyde lyase. *J. Mol. Catal. B: Enzym.* **2006**, *38* (1), 43−47.
(50) Dünnwald, T.; Demir, A. S.; Siegert, P.; Pohl, M.; Müller, M. Enantioselective synthesis of (*S*)-2-hydroxypropanone derivatives by benzoylformate decarboxylase catalyzed C−C bond formation. *Eur. J. Org. Chem.* **2000**, *2000* (11), 2161−2170.
(51) Bornadel, A.; Hatti-Kaul, R.; Hollmann, F.; Kara, S. A bi-enzymatic convergent cascade for ε-caprolactone synthesis employing 1,6-hexanediol as a 'double-smart cosubstrate.'. *ChemCatChem* **2015**, *7* (16), 2442−2445.
(52) Sehl, T.; Hailes, H. C.; Ward, J. M.; Wardenga, R.; von Lieres, E.; Offermann, H.; Westphal, R.; Pohl, M.; Rother, D. Two steps in one pot: Enzyme cascade for the synthesis of nor(pseudo)ephedrine from inexpensive starting materials. *Angew. Chem., Int. Ed.* **2013**, *52* (26), 6772−6775.
(53) Sattler, J. H.; Fuchs, M.; Tauber, K.; Mutti, F. G.; Faber, K.; Pfeffer, J.; Haas, T.; Kroutil, W. Redox self-sufficient biocatalyst network for the amination of primary alcohols. *Angew. Chem., Int. Ed.* **2012**, *51* (36), 9156−9159.
(54) Dicks, A. P.; Hent, A. Atom economy and reaction mass efficiency. In *Green Chemistry Metrics: A Guide to Determining and Evaluating Process Greenness*; SpringerBriefs in Molecular Science; Springer International Publishing: Cham, Switzerland, 2015; pp 17−44..
(55) Sheldon, R. A. Fundamentals of green chemistry: efficiency in reaction design. *Chem. Soc. Rev.* **2012**, *41* (4), 1437−1451.
(56) Woodley, J. M. New opportunities for biocatalysis: making pharmaceutical processes greener. *Trends Biotechnol.* **2008**, *26* (6), 321−327.
(57) Wachtmeister, J.; Mennicken, P.; Hunold, A.; Rother, D. Modularized biocatalysis: immobilization of whole cells for preparative applications in microaqueous organic solvents. *ChemCatChem* **2016**, *8* (3), 607−614.
(58) Lingen, B.; Grötzinger, J.; Kolter, D.; Kula, M.-R.; Pohl, M. Improving the carboligase activity of benzoylformate decarboxylase from *Pseudomonas putida* by a combination of directed evolution and site-directed mutagenesis. *Protein Eng., Des. Sel.* **2002**, *15* (7), 585−593.

DOI: 10.1021/acssuschemeng.8b02107
ACS Sustainable Chem. Eng. 2018, 6, 11819−11826